



## **Experimental measurements on Tekna“PlasmaSonic” High Enthalpy Ground Testing Facilities using 350 kW ICPT plasma torch to reproduce re- entry conditions of space vehicles**

*Y. Lakaf1, S. Xue1,*

*1Tekna Plasma Systems, Department of Innovation and R&D technologies, Sherbrooke, Québec, Canada*

### **Abstract**

This paper describes an experimental investigation of plasma jet properties on PlasmaSonic 350 kW Inductively Coupled Plasma Tekna torch, operated in the Ground Testing Facility System, designed for thermal material protection research and experimental studies of aerodynamics heating effect, under high enthalpy flow testing. The ICPT-350 kW can be operated from 0.3 to 5 bar torch pressure and develops an enthalpy flow conditions up to 31 MJ/Kg. Various experimental measurements such as enthalpy, heat flux and sample surface temperature are presented and discussed.

**Keywords:** *Tekna ICPT 350 kW, Supersonic flow, High Enthalpy flow, intrusive and non-intrusive techniques.*

### **1. Introduction**

The plasma wind tunnel consists of a stationary test facility in which a high enthalpy flow is generated using plasma generator and a pumping station to reproduce the re-entry conditions of space vehicles.

The ground testing facility using Inductively Coupled Plasma Torch 350 kW, (ICPT) are widely used in experimental investigations of heat shield materials and thermal protection systems (TPS) that the external envelop of space shuttle are faced.

The main purpose of this installation is to reproduce those conditions where material samples are tested under high enthalpy flow such as aerodynamic heating effect under supersonic flow that the capsules may be faced during re-entry to the atmosphere. For this purpose, a complete study and simulation of the physical phenomena, must be studied and completely understood at the ground facility. On this paper we are presenting an experimental measurements of plasma physical parameters compared to the numerical model calculations with a measurement of inner and outer surface temperature of the graphite material sample.

### **Nomenclature**

ICPT – Inductively coupled plasma torch  
HFT – Heat Flux Transducer  
T – Temperature  
HFT – Heat flux transducer  
CFD – Computational fluid dynamics  
 $P_{i2}$  – Stagnation pressure

$P_1$  – Static pressure  
 $\lambda$  – Wavelengths  
° – degree Celsius  
 $h_i$  – Inlet enthalpy  
 $h_e$  – Exit enthalpy  
GTFS – Ground Testing Facility System

### 1.1 ICPT-350 kW capabilities

The proposed ICPT-350 plasma system will have the ability to perform thermal tests between 10-1000 mbar chamber pressure with 100 % air. Exhaustive instrumentations are also provided with the system allowing characterization of the plasma flow and heat flux on the sample.

The performance testing of insulation thermal system such as the improvement of flow characteristics on this plasma tunnel system, passes by a design of high-quality equipment and high control and regulation such as 1) Tekna ICP plasma torch 2) Test chamber 3) Supersonic diffuser 4) Vacuum system 5) Heat exchanger 6) Power supply 7) Advanced control system.



**Fig 1.** Tekna ICPT 350 kW Tunnel

### 2. Tekna 350kW-ICPT torch

Tekna torch used for 350kW ICPT system, is mounted inside a Faraday cage, avoiding propagation of electromagnetic waves outwards, and it allow various configuration of subsonic and supersonic nozzles installation. Both torch and nozzles are mounted on separate supports to facilitate the change of nozzles and/or the installation of quench sections when needed.

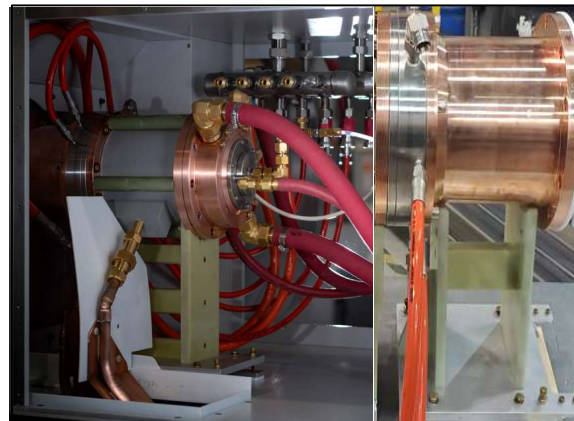


**Fig 2.** Tekna 350kW-ICPT torch with nozzle

Various combination of gases has been experimented and are summarized in table 1.

Depending about the mixture of gas used, the power level varied from 300KW to 350kW.

**Table 1.** The specification of gas mixture experimented in the 350kW-ICPT

Air	Air/Ar	N2/H2	CO2
100%	95%/5%	98%/2%	100%
9.7 g/s	4.2 g/s	10.2 g/s	7.8 g/s

Tekna’s induction plasma torches are based on a patent protected ceramic technology developed in the 80’s. This induction plasma is specifically designed to operate at high energy density and can operate under a wide range of conditions with oxidizing, reducing and inert plasma gases. This allows a high purity process since the plasma is not in contact with any electrodes.

The main parts of the Tekna torch are 1) a copper coil embodied inside the resin constituting a body of the torch. Therefore, no copper is facing the plasma in the plasma discharge zone; 2) a ceramic confinement tube, ensuring a high-density energy; 3) Advanced aerodynamic gas sheathing design and 4) the central gas used for generating the core of the plasma. The water cooling flowing through the copper coil of the torch is running to dissipate the heat produced in operation. The coil is wrapping the water-cooled copper diffuser disposed on the central of the torch, in replacement of the Quartz tube, for the plasma generation. This later, is used in replacement of Quartz tube, for systems that operating power is over 40kW. The water copper diffuser provides more stability of plasma mainly at high pressure operation and it lasts longer.

### 2.1 Facility sub-systems

The experimental campaign has been conducted inside a vacuum chamber mounted with various windows, disposed adequately to provide the best viewing of the plasma plume and sample surface measurement using a non-intrusive technique. Inside the vacuum chamber of 1.8 m x 1.2 m, an automatized 3 axis rotary arms, for holding samples, is disposed on the left side of the catch cone. It has 4 cooled arms rotating in 280° to allow in the same test having various physical parameters measured. (Fig. 3)

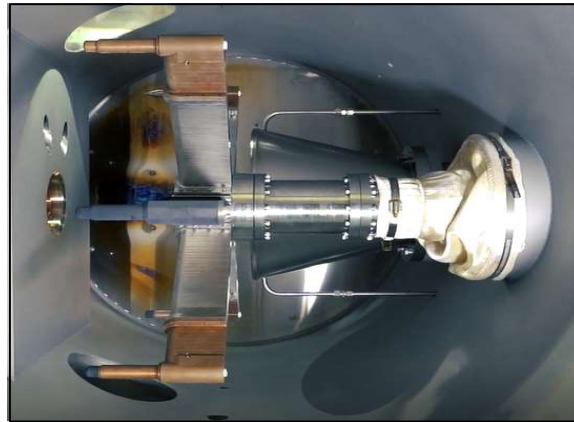


**Fig 3.** Catch cone and rotary arm with probes for plasma plume and material characterization.

The complete features of the displacement system are disposed outside of the vacuum chamber to extend the lifetime of various component which may be deteriorated because of plasma radiation and heating effect. No cooling duct or wire are visible inside the vacuum chamber.

The exhaust of hot gas is assured by a supersonic diffuser, starting from the catch cone, with an appropriate length to contain the oblique shock, followed by a water-cooled heat exchanger, toward a vacuum system with a capacity of 85 g/s at 50 mbar.



**Fig 4.** Supersonic Diffuser with heat exchanger

The experimental investigation and development of novel thermal barrier material passes by a characterization and measurement of plasma jet properties under various conditions of enthalpy and velocity. The experimental measurements of plasma jet parameters such as: the specific enthalpy, plasma temperature, velocity, and heat flux have been achieved using intrusive measurement techniques. This method of plasma characteristics is based on the suitable design of mechanical probes able to sustain high thermal energy and forces and are represented in the fig. 5.

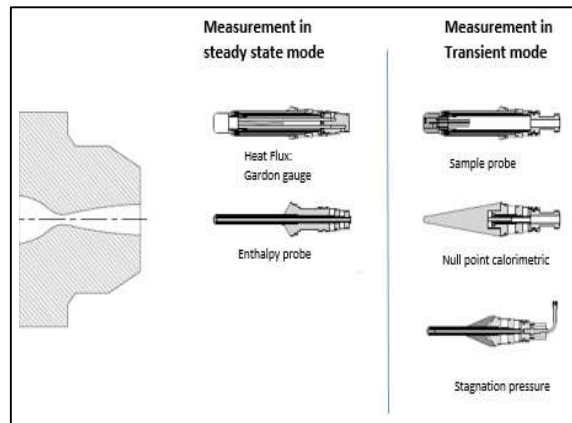


**Fig 5.** Various Tekna probes used for plasma jet characterization.

The fact that the samples manipulator is mounted with 4 cooled arms, on which different probes are installed, allow to have simultaneous measurement of physical parameters of the plasma jet, described above, during the same test. The 3 axis rotary arms can achieve measurement close to nozzle exit plan and few centimetres downstream of the plasma jet (Fig. 3). The several points of measures obtained on the jet axis and its surrounding, allow to have various point of measurement and are necessary for:

- Validation of CFD code and assumptions in plasma Arc tunnel.
- Qualification and development of novel thermal barrier materials using various measurement devices.

The results of the measurements achieved are presented and discussed on this paragraph.

### 3.1 Enthalpy using supersonic Tekna probe

The Tekna supersonic enthalpy probe is used for local plasma enthalpy, plasma temperature, plasma velocity and Mach number measurements. [1]

The main advantage of Tekna supersonic enthalpy probe is designed to have the measurement of the static pressure of the flow and the total pressure on the same probe as shown on the fig. 6.

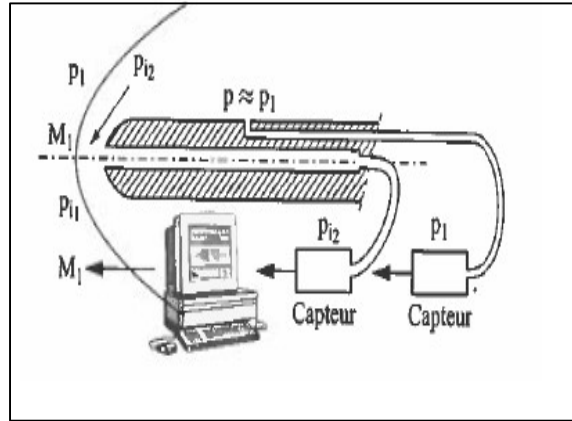


**Fig 6.** Tekna supersonic enthalpy probe design

This design allows reducing the uncertainty of measurement which may occur by using various probes, such as aerodynamic wedge probe used to measure Mach number or pitot tube used to measure dynamic pressure [2], that are reported on literature, and which can lead to perturb the plasma differently because of their different shapes. The hole on Tekna probe, measure the static pressure after shock, when other instruments are considering a static pressure to be equal to the pressure inside the vacuum chamber which can increase errors. Indeed, the static pressure of the plasma jet, in supersonic mode, is not constant and vary along the jet axis. This is even more important when the supersonic flow impact the enthalpy probe which result in occurring a bow shock on the nose tip of the probe and lead inevitably in the static pressure variation.

The post-shock static pressure described by [3] measures the static pressure after a shock generated on the nose tip of enthalpy probe by using a separate probe. Even if this probe tends to reproduce the shock it has the disadvantage to use 2 different probes which inevitably leads to increase error in measurements. The Tekna enthalpy probe measure static and stagnation pressure using the same probe.

#### 3.1.1 Enthalpy measurement principle

The local enthalpy of the plasma can be derived from an energy balance applied to the cooling water flowing through the probe and the gas sample extracted from the plasma. To determine the external heat load transferred to the probe, 2 modes of measurements are performed following a) Tare mode: without sample gas flow and b) Sample mode: with a sample gas flow from the plasma through the probe. [1]

The plasma enthalpy is given by the equation:

$$h_i = h_e + \frac{\dot{m}_w}{\dot{m}_g} C_{p_w} (\Delta T_{\text{sampling}} - \Delta T_{\text{tare}})_w \quad (1)$$

Where  $h_e$  is the enthalpy measured at the temperature of gas exit from the probe. The  $\dot{m}_w$  and  $\dot{m}_g$  are respectively mass flow rate of water and gas sampled inside the probe.  $\Delta T$  represents the cooling water temperature elevation measured during both modes.

Having obtained the gas enthalpy value, the temperature can be calculated using tabulated enthalpy data for pure gases as function of temperature.

For gas mixtures, the specific enthalpy must be computed using standard mixing rules for each specific gas mixture as:

$$h_{\text{mix}}(T) = \sum_{i=1}^n x_i h_i(T)$$

Where  $h_i(T)$  is the specific enthalpy of gas  $i$  present in the mixture of gases at temperature  $T$ .

In tare mode, without sample gas flow, the probe is used to measure a stagnation pressure and static pressure acting as static Pitot tube. The second hole of the probe, dedicated for static pressure flow measurement, is disposed on rear back of the probe, downstream of the shock wave.

The equation used to determine the Mach number, in supersonic plasma jet, is called Rayleigh formula and is expressed as:

$$\frac{P_{i2}}{P_1} = \left[1 + \frac{2\gamma}{\gamma+1}(M_1^2 - 1)\right]^{\frac{-1}{\gamma-1}} \left[1 - \frac{2}{\gamma+1}\left(1 - \frac{1}{M_1^2}\right)\right]^{\frac{-\gamma}{\gamma-1}} \left(1 + \frac{\gamma-1}{2}M_1^2\right)^{\frac{\gamma}{\gamma-1}} \quad (2)$$

The pressure ratio  $\frac{P_{i2}}{P_1}$  is measured experimentally via dedicated gauges connected to both holes of the probes as shown by the fig. 6. [4]

The Mach number is computed by solving a Rayleigh equation (2).

### 3.1.2 Enthalpy measured with 350 kW ICPT

The table 2 shows the plasma conditions of the enthalpy measurement in a supersonic and subsonic flow. Various plasma conditions were tested as described in table 1.

**Table 2. The Plasma conditions**

Plasma cond.	Power	Ch. pressure	g/s	P torch
Nozzle A (*21.8mm)	350kW	93.4 mbar	9.67*	0.5bar
Nozzle B (*7.48mm)	300kW	105.8 mbar	15.0 **	4.7bar

\*100Air, \*\* Air/Ar

The pressures inside the torch vary from 0.4 bar to 5 bar respectively following conditions A and B described on the table above. On this paper, we are reporting only the condition used with a nozzle A at 350kW-100%Air.

The probe distance, from the exit plan of the nozzle, has been fixed to 120 mm to 148.4mm. The stagnation enthalpy has been measured in the center line of the plasma only. The probe has been aligned with the center line of the nozzle (Fig. 7).

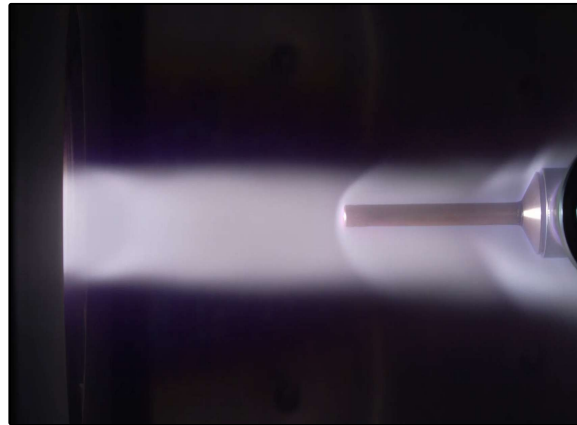


**Fig 7.** Tekna enthalpy probe inside the plasma plume



The stagnation enthalpy measured using Tekna supersonic probe, has been compared with the enthalpy calculated using a numerical model and the total enthalpy deduced from the heat balance. The 4 parts constituting the torch are computed to measure the energy lost by those sections to the water cooling. By extracting the total energy lost before and after nozzle, to the water cooling, the efficiency of the torch is determined. Therefore, the enthalpy can be estimated on the nozzle according to the equation:

$$P_{elec} - \dot{Q}_{water} = \dot{m}_{gas} \Delta H \tag{3}$$

The figure 8 a-b shows the stagnation Enthalpy and Stagnation pressure measured by the Tekna probe compared to the enthalpy calculated using a numerical model. The average enthalpy calculated from the heat balance is reported on the same graph at the position  $x = 0$  mm corresponding to the exit plan of the nozzle.

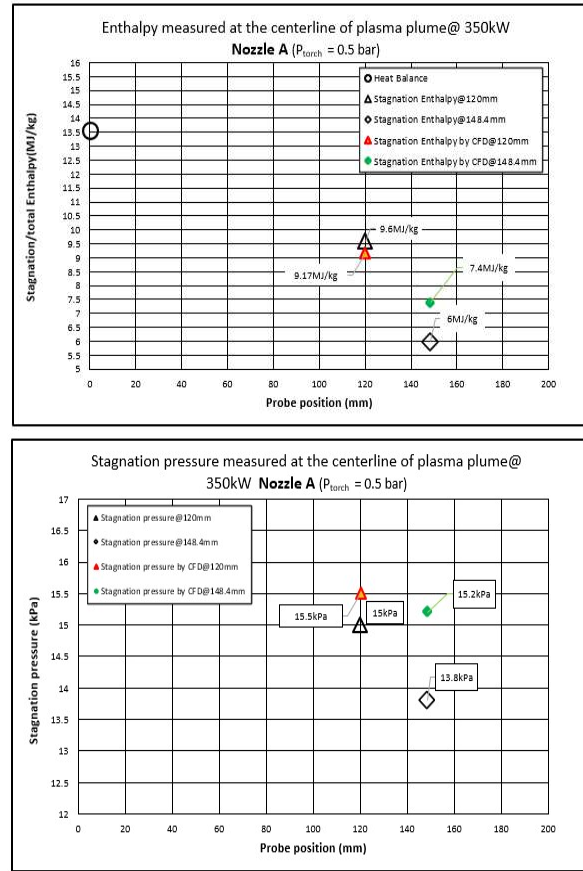


**Fig 8.** a) Enthalpy results using Tekna enthalpy probe, numerical model and calorimetric balance, b) Stagnation pressure in kPa.

The Stagnation enthalpy measured experimentally by Tekna probe, with a nozzle A at 0.5 bar torch pressure, is 9.6 MJ/kg when the CFD model calculated 9.17 MJ/kg for a stand-off distance 120 mm from exit plan of the nozzle, and it is 6 MJ/kg at a stand-off distance of 148mm and CFD calculates 7.4MJ/kg. If both experimental measurements and CFD are close each to other, the position of 120 mm, shows a deviation of 4.7%, which is good, but at position 148 mm, the deviation climb to 18.9%. This may be caused by a small deviation from the centerline of the jet when we moved back the arm (backward).

Indeed, it has shown on the CFD model, that a deviation of 0.5 mm from the central line of the plasma, can lead to such deviation, when on the CFD model construction, the Tekna enthalpy probe geometry is aligned with a pixel precision with the torch center line, Fig. 9.

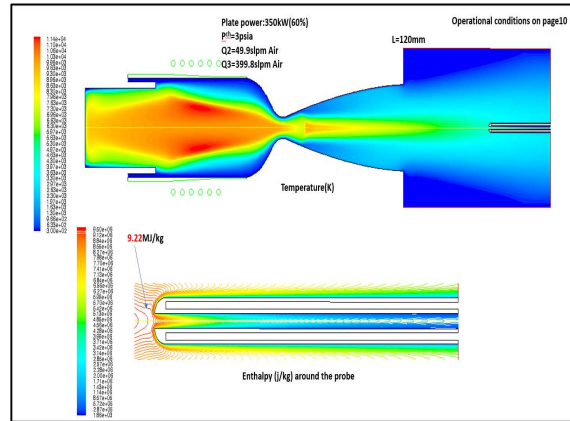


**Fig 9.** Tekna enthalpy probe as aligned on the CFD model

The stagnation pressure measured experimentally shows a deviation less than 4% with the stagnation pressure estimated numerically, for the stand-off distance of 120mm. For the stand-off distance of 148.4mm the experimental measurement presents deviation of 10.2 %. The experimental measurement presents a good match with a CFD model and lead to conclude that the Tekna enthalpy probe can be used to estimate both stagnation/total and stagnation pressure with a reasonable error.

The fig. 10 present the experimental measurement and numerical results of plasma temperature, and Mach number calculation, using a Tekna enthalpy probe for a nozzle A at 0.5bar torch pressure and operating power at 350 kW.

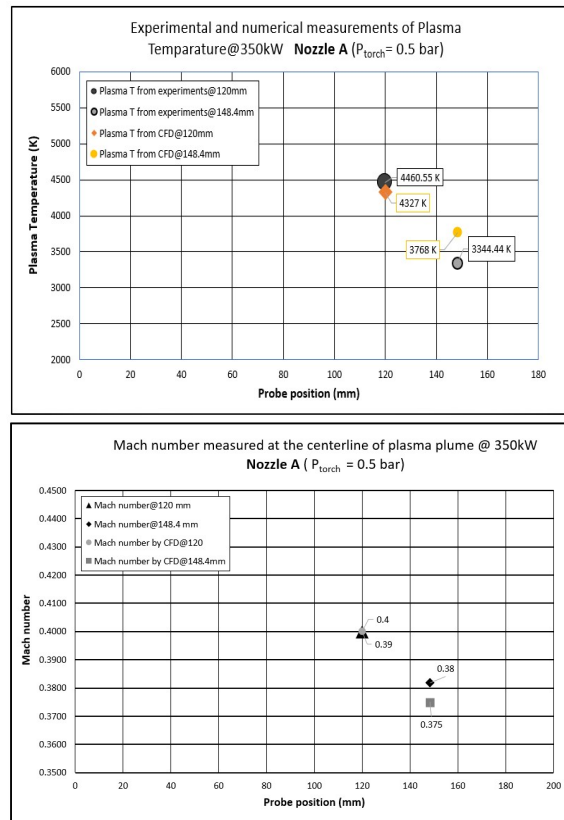


**Fig 10.** a) Temperature and b) Mach number calculated from Tekna enthalpy probe and CFD model.



The plasma temperature is deduced from the gas mixture table created, at the specific chamber pressure. Knowing the enthalpy measured experimentally, via the probe, the plasma properties are then deduced from a pre-programmed table of various gases starting from 200K to 22000K. The experimental enthalpy is compared to the one existing on the table, and the rest of the physical parameters are deduced from the table such as: density, temperature, Gamma, electrical conductivity, and viscosity.

The deviation between both temperatures calculated experimentally and numerically, shows a deviation of 3% to 11% for both positions of 120 mm and 148.4 mm, respectively. The same constatation on the Mach number calculation is done on both positions of 120mm and 148.4mm. The deviation for both positions does not exceed 3%.

Even if some results present a deviation of 18%, between experiment and numerical analysis, this remains a very good and interesting design to investigate and measure plasma parameters under supersonic and subsonic flow condition.

### 3.2 Heat flux measurement in steady state

The stationary heat flux probes have been used to measure heat flux at 350 kW of the ICPT system. The stationary probe is water cooled and mounted with a heat transducer which is cooled separately and called Gardon gage and described well in the literature [2].

The probe mounted with the transducer at its nose tip is aligned with the center line of the plasma jet using laser alignment system

#### 3.2.1 Heat flux measurement using Gardon gage:

The measurement of the heat flux load result from the conversion of a linear 0-10mV output directly to a proportional net absorbed heat transfer rate to the sensing tip at the stagnation point. The conversion of signal to a net absorber heat transfer is given by a calibration certificate provided by the manufacturer.

The Gardon transducer is chosen with the same geometry of the material to be tested to measure the plasma heat flux with the same perturbation. The Gardon probe is aligned with the center line of the plasma and disposed at  $x = 120$  mm and  $X=148.4$ mm from the exit plan of the nozzle (Fig. 11). The measurement was performed under subsonic plasma flow with torch operating at 0.5 bar (Nozzle A).

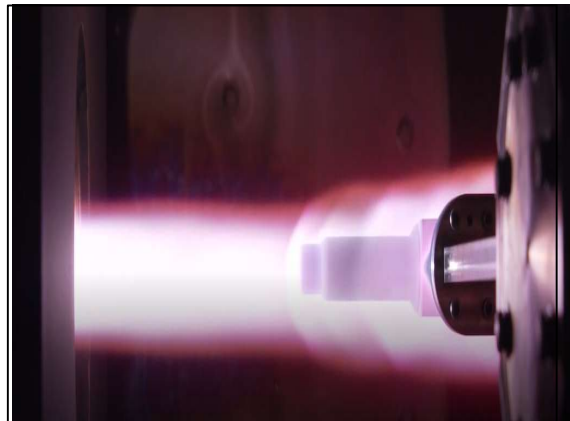


**Fig 11.** Tekna heat flux probe mounted with Gardon gauge inside the plasma plume of P torch= 0.5bar.

The Gardon gauge probe has been inserted inside the plasma plume when the chamber pressure was at 95 mbar. The Heat flux measured experimentally was not possible to be verified with the CFD model as it is

very hard to estimate the heat flux in none accorded jet as it is hard to reproduce the shocks that are generated in a none accorded jet.

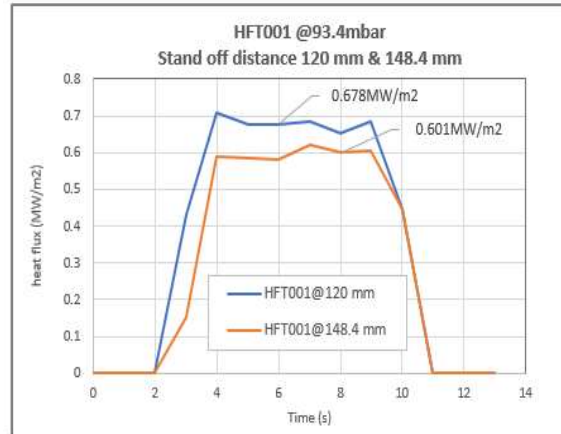


**Fig 12.** Heat flux measurement in MW/2 obtained experimentally.

### 3.2.2 Surface temperature measurement using: IR camera, Pyrometer and Fast Response Thermocouple

The non-intrusive diagnostic plasma techniques have been conducted via different windows disposed on the vacuum chamber. Those techniques are used for front material surface temperature measurement, performed using an optical measurement instrument such as IR camera and Pyrometer. A very thin thermocouple of 0.02" in diameter is inserted inside the material. Thus, the results obtained with fast response thermocouple are reported with the surface temperature measurements of the material using optical techniques. [5]

The main objective from those techniques is to study the ablative materials at high heat flux levels and provide a database on precise information about the materials to be characterized and developed for thermal barrier protection used for re-entry of space shuttle. Both IR camera and pyrometer used on this experimental measurement of surface temperature behavior are operating in the close spectral range near infrared to avoid measuring the light coming from the plasma. The IR camera is operating in spectral range of 0.9 to 1.7  $\mu\text{m}$ . It is provided with 2 calibrated intensity filter allowing measurement from 500-1200°C and from 1200-3000°C respectively.

The pyrometer used is operating bi-chromatic which measures the intensity of infrared radiation at two different wavelengths ( $\lambda_1 = 950 \text{ nm}$  and  $\lambda_2 = 1050 \text{ nm}$ ) at the same time. The ratio of these two intensities is proportional to the temperature. Thus, a two-color pyrometer measurement is not influenced by emissivity changes or obstructions within the sight path such as dust or water vapor.

Both optical techniques are mounted at the external windows of the vacuum chamber and disposed at the same distance from the target.

The thermocouples are chosen to be as thin as possible, (fig. 13) in the range of less than 1-millimetre diameter, to be as less intrusive as possible to the material to be characterized. It is mounted inside the material and are aligned with the material center. The upper one (FTT003) is around 5mm from the nose tip.

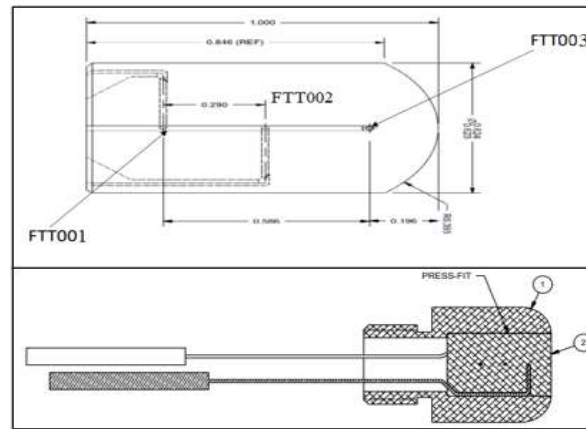


**Fig 13.** Fast thermocouple as used on the graphite sample.

As the response time of the 3 thin thermocouples of type K, are very fast, we are using a high-speed data acquisition that have 8 insulated channels and can read the time response of each thermocouple in nano seconds. As the sample probe is facing a high heat flux at its front, this results in the fast-rising temperature of the thermocouple and can leads inevitably of damaging the thermocouple after certain or unique use. The high-speed data acquisition device is set in 1 microsecond for a maximum duration of 10 seconds. The measurements are presented on the fig. 14.

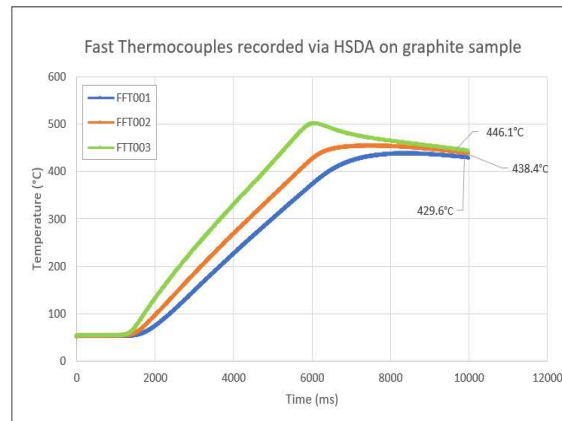


**Fig 14.** Fast thermocouple response inserted inside a graphite sample at 350kW with Nozzle A.

From the Fig. 15 a) and b), the surface temperature measured by the pyrometer is 510 °C and the temperature measured by the IR camera delimited by the blue circle (1) shows a maximum temperature of 570°C. The software also allows to determine in the delimited circle the minimum and average temperature estimated to be 570.2°C and 572.9°C respectively.

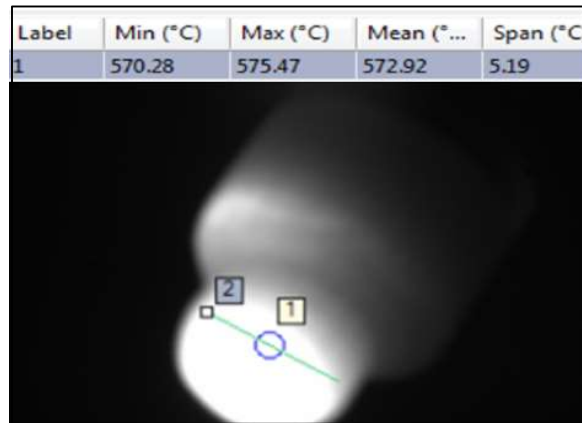


**Fig 15.** Surface temperature measurement of sample using a) Pyrometer b) IR camera.

The blue circle, shown on the Fig. 16 represent the red laser sport done by the pyrometer during alignment on the Tekna sample probe. This is very important step to be performed by the operator before to be able to compare both measurements.

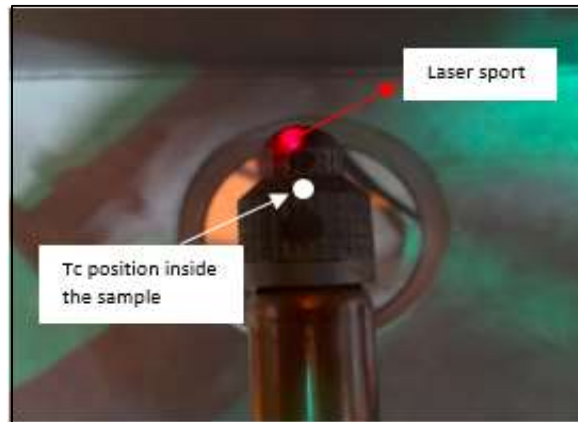


**Fig 16.** Laser sport alignment using pyrometer laser to determine the point of comparison with IR camera measurement.

Considering the minimum, maximum and average temperature measured by the IR camera, in all cases, the deviation comparing to the surface temperature measured by the pyrometer is not exceeding 10%.

The information resulting from this experiment is that the graphite material tested present a temperature difference of 64 °C between the inner and the outer surface. Those thin thermocouple have a short life duration if they let for a long time. This technique of surface measurement using a thermocouple is validated as a method of inner sample surface temperature measurement. The information of inner temperature using thin thermocouples and external surface temperature using IR camera and pyrometer allows to determine the thermal conductivity of the material to be used.

### 3.3 Erosion testing system

Tekna PlasmaSonic ICPT 350 kW can be provided with a high erosion testing configuration. This configuration is dedicated to the material testing and deposition or coating. This configuration include: 1) Independent coating and erosion 3 axis manipulator, 2) Powder feeder, 3) particle trap and filtration system. 4) Curved duct interlocked with the powder feeder. This interlock avoid sending powder if the system is configured in Aerospace setup. (Fig. 17)



**Fig 17.** Particle trap and filtration system with an S duct to deviate the powder to the filtration system.

After the particle trap system, the gases are directed to the heat exchanger, and then to the vacuum system.

The high erosion testing configuration is provided with a Laser based velocity measuring system for particle erosion and coating experiments with spray pattern trajectory, for measuring the instantaneous global velocity field of particle flowing in the plasma plume. This system is also commonly called PIV (Particle Imaging Velocimetry). The PIV technique comes with 1) Lighting source which consist on the double pulse Nd-YAG laser, 2) High resolution monochrome camera of 2048x1700 pixels 3) Acquisition and analysis software.

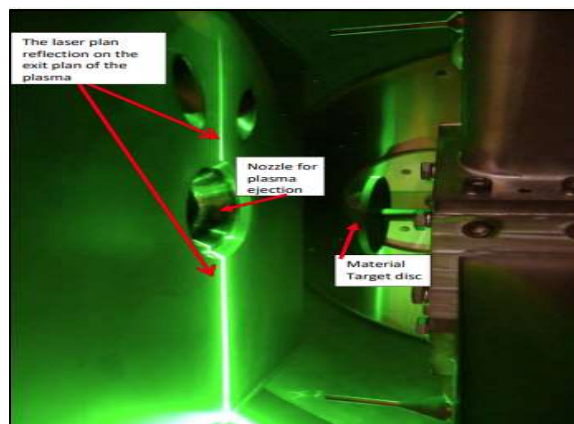


**Fig 18.** The laser plan as generated inside the room chamber

The light plan generated, of about few mm thickness, where the particles flow through it, will diffuse the light (Mie scattering formulation). The trace images of light scattering of particles are collected at the  $90^\circ$  to laser emission source. Two successive images are saved in the interval time of few  $\mu$ s (following the particle speed in plasma jet). The laser is pulsed (6ns) to freeze an image of the flow. With two successive frames of the same particles, being moved in the plane of light, the instantaneous velocity field is then calculated.

Compared to other techniques, it has the advantage to provide the map of the instantaneous velocity field of the flow (flow structures, swirls, form of the jet, areas of mixtures etc...). It allows determining the velocity field's statistics spatially (average on several local vectors) and temporally (average on several instant velocity fields). The PIV has been dimensioned to be able to measure the velocity of particle in the range of 50 m/s to 900 m/s.

The fig. 19 a) and b), shows the particle as flowing on the plasma jet during coating and erosion testing, respectively. The light plan generated by the laser and detected by the high-resolution camera eliminate the particles.

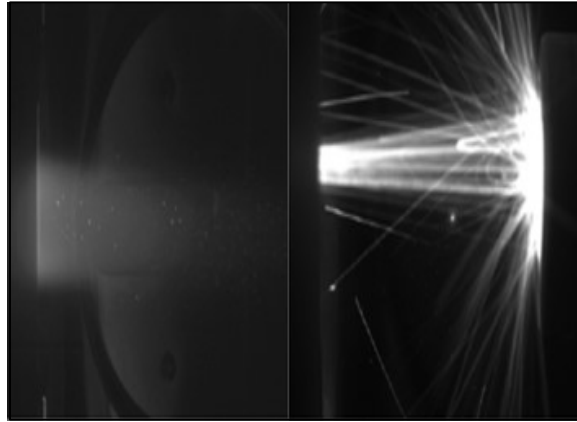


**Fig 19.** The path during a) coating and deposition and b) erosion testing as detected by the PIV system.

The software integrated with the PIV system, allow the acquisition and the treatment of the images to calculate the velocity of the powder. It allows to calculate the rebound velocity that is important during erosion testing. The calculation of the velocity is shown on fig. 20. The axial velocity on the sense of the flow is estimated at 221.66 m/s.



**Fig 20.** Velocity calculation of particle during the erosion testing.



## Conclusion:

The measurements of plasma physical parameters have been conducted using a various intrusive instrument and compared to the CFD model calculation. The measurements have been limited at the center line of the plasma. Indeed, in the center line of the plasma, the thermal equilibrium is approached and/or reached. Therefore, the effect of non-equilibrium because of low pressure and supersonic flow are less significant. The CFD assumption are validated, and the calculation obtained has reinforced our experimental campaign and are in accordance with our results and assumption of torch and nozzle designs. This also demonstrate the robustness of our probe design, and their operation under high pressure and thermal stress conditions. The deviation between both methods, is contained within a reasonable percentage for the measurement under high enthalpy flow conditions.

These results can serve as an interesting database for experimental measurements in this type of installation and in our knowledge, there is not much experimental data reported in such facility.

Using non-intrusive instruments such as IR camera and pyrometer to measure the sample surface temperature has shown a very interesting results. The measurements resulting from both techniques have been correlated and present a similarity on the target point. Finally, it has been demonstrated that using some experimental set-up and rules before starting plasma, the data collected under high enthalpy and velocity flow, can be used, with confident, to characterize and qualify the material to be used as a thermal barrier material on aerospace shuttle vehicles.

## References

- Journal article

1. RAHMANE, M. SOUCY, G. BOULOS, M.: Analysis of the enthalpy probe technique for thermal plasma diagnostics. *Rev.Scl.Instrumen.Vol.66, No.6, (Jun.1995)*.
2. AUWETER-KURTZ, M., FEIGL, M. WINTER, M.: Diagnostic Tools for Plasma Wind Tunnels and Re-entry Vehicles at the IRS. Rhode-Saint-Genkse, Belgium, (25-29 Oct.1999).
3. J.-L. DORIER, J.-L. JODOIN, B., GINDRAT, M.: A novel approach to interpret enthalpy probe measurements in low pressure supersonic plasma jets., *Proc. of 16th International Symposium on Plasma Chemistry, Taormina, Italy, (22-27 Jun. 2003)*.
4. C. O. ASMA, C-O. HELBER, B. Infrared thermography measurements on ablative thermal protection systems for interplanetary space vehicles. *10th International Conference on Quantitative InfraRed Thermography, Québec, Canada, (30 Jul. 2010)*.

- Book chapter 7

5. ANDERSON, J-D.: *Fundamental of aerodynamics. 4th edition*